ON THE USE OF LANGEVIN EQUATIONS IN DISLOCATION PATTERNING AND DEFORMATION INHOMOGENEITIES

Peter HÄHNER

European Commission, Institute for Advanced Materials, TP 750, Joint Research Centre, I-21020 Ispra (Va), Italy; e-mail: peter.haehner@jrc.it

Abstract. Dislocation dynamics theories of spatio-temporal structure formation during plastic flow encounter the problem of dealing with the long-range dislocation interactions. The basic idea of the stochastic dislocation dynamics presented here consists in accounting for the fluctuations of the local effective stress and of the plastic shear strain rate that are caused by transient dislocation interactions during glide. The correlation functions of the effective stress and of the strain rate are related to the strain-rate sensitivity and the mechanical power dissipation using an effective medium approach. Plastic flow properties may then be described in terms of stochastic differential equations of the Langevin type. The applications presented refer to (i) the random aspects of the macroscopic plastic strains and tensile stresses, and (ii) the evolution of the dislocation densities pertinent to noise-induced dislocation patterning.

Key words: plasticity, dislocations, stochastic dynamics, pattern formation, noise-induced transitions.

1. INTRODUCTION

Dislocation dynamics approaches to plastic flow properties of metals and alloys are known to offer several advantages as compared to traditional continuum mechanics theories: (i) they may provide physical justifications of the constitutive viscoplastic laws used in continuum mechanics, (ii) they may give access to the characteristic length and time scales that are important for modelling the spatio-temporal aspects of plastic deformation and, obviously, (iii) dislocation dynamics modelling is indispensable for understanding the spontaneous formation of dislocation patterns which, being outstanding examples of self-organization in

complex systems far from equilibrium, have stimulated much theoretical work during the last decade [1–3].

In practice, however, fundamental problems inherent in dislocation dynamics approaches are due the long-range interactions between dislocations. They are the reason why in dislocation dynamics one is dealing with complex systems where the length scales are not clearly separable. As depicted schematically in Fig. 1, the correlation length ξ over which mobile dislocations may behave in a collective way is of the same order of magnitude as the characteristic wavelength of the spontaneously emerging dislocation patterns. That this situation is somewhat peculiar can be seen from a comparison with other, theoretically much better understood examples of pattern formation, such as chemical patterning (Fig. 2). Here patterns show up on a macroscopic scale (10^{-3} m) that is well separated from the microscopic scale (10^{-9} m) where thermal fluctuations and the discreteness of particles become appreciable. Therefore, patterning phenomena can be described theoretically in terms of *deterministic* continuum approaches of the reaction–diffusion–transport type. The situation is quite different with dislocation dynamics, where fluctuations and the discreteness of dislocations manifest themselves on the same mesoscopic scale (10^{-6} m) that is characteristic of patterning. Under these circumstances it seems safe to resort to some type of *stochastic* approach, in order to get an idea to what extent the fluctuations average out and whether fluctuations may induce qualitative changes in dislocation dynamics that can be associated with patterning.
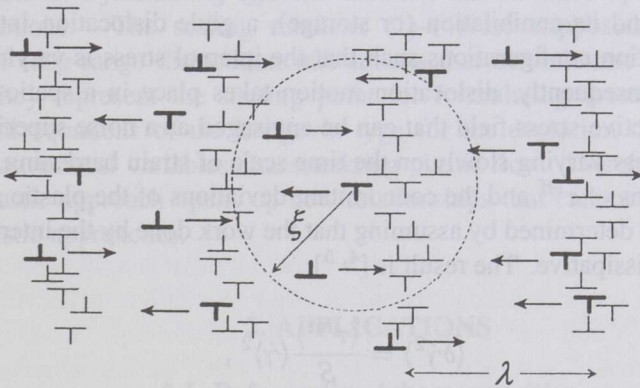
Fig. 1. Illustration of the correlation length ξ of mobile dislocations ($\perp$ and $\top$ signs) and of the characteristic wavelength λ of an emerging pattern of sessile dislocations ($\perp$ and $\top$).

To this end, let us consider the effective shear stress (driving stress) $\tau^{\text{eff}} = \tau^{\text{ext}} - \tau^{\text{int}}$ that acts on a gliding dislocation. It is given by the external resolved shear stress τ^{ext} and the long-range internal shear stress τ^{int} (back stress) exerted by other dislocations. During the time passing between its generation (or

65
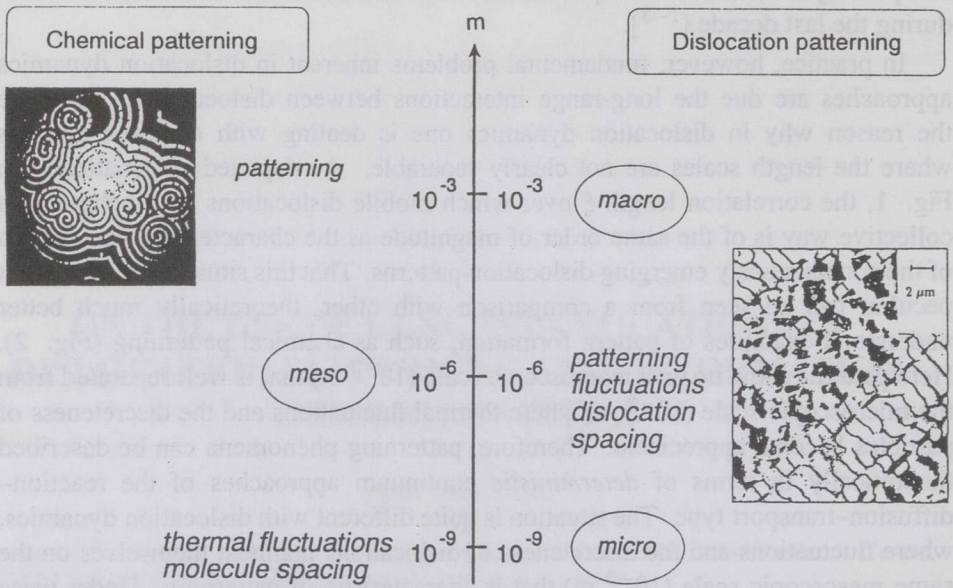
Fig. 2. Comparison of the length scales involved in chemical patterning (e.g., the spiral waves associated with the Belousov–Zhabotinski reaction) and dislocation patterning (e.g., the persistent slip band and matrix structures occurring during cyclic plastic deformation). In the latter case the mesoscopic scale where fluctuations show up is important.

mobilization) and its annihilation (or storage), a glide dislocation interacts with various dislocation configurations such that the internal stress is varying along its glide path. Consequently, dislocation motion takes place in a spatio-temporally fluctuating effective stress field that can be envisaged as a noise superimposed on the external stress varying slowly on the time scale of strain hardening. The mean square deviations of τ^{eff} and the concomitant deviations of the plastic shear strain rate $\dot{\gamma}$ are easily determined by assuming that the work done by the internal stresses is completely dissipative. The result is [4, 5]:

$$\langle \delta \dot{\gamma}^2 \rangle = \frac{\langle \tau^{\text{int}} \rangle}{S} \langle \dot{\gamma} \rangle^2 , \tag{1}$$

$$\langle (\delta \tau^{\text{eff}})^2 \rangle = S \langle \tau^{\text{int}} \rangle . \tag{2}$$

Equations (1) and (2) relate the local fluctuations to the strain-rate sensitivity $S = \partial \langle \tau^{\text{eff}} \rangle / \partial \ln \langle \dot{\gamma} \rangle$ which represents the dynamic response function, and to the mechanical power dissipation which is governed by the ensemble average of the internal stress as experienced by the glide dislocations: $\langle \tau^{\text{int}} \rangle$ ("fluctuation–dissipation theorems of plastic flow").

In the direction normal to the dislocation glide planes, a correlation length ξ of fluctuations can be introduced which formally establishes a scale of "coarse graining" while, physically, it corresponds to the characteristic range of dislocation interactions. As a discussion of this correlation length has been given elsewhere [4–6], we only point out that ξ is defined from a dynamic point of view by noting that two dislocations interact strongly enough to glide in a correlated way, only if their interaction stress exceeds the random stress fluctuations exerted by other dislocations. This gives the following scaling law for the correlation length [4–6]:

$$\xi = \frac{\mu b}{4\pi\sqrt{\langle(\delta\tau^{\text{eff}})^2\rangle}} = \frac{\mu b}{4\pi\sqrt{S\langle\tau^{\text{int}}\rangle}}, \tag{3}$$

where μ denotes the shear modulus and b the length of the Burgers vector. It is interesting to note that a random array of *static* dislocations in an infinite medium does not possess a finite interaction range (cut-off) as a consequence of the $1/x$ type interaction law [7]. The finite correlation length ξ defined here, however, derives from *dynamic* arguments.

Correlations are limited in time due to dislocation immobilization (storage or annihilation). This is expressed by the following scaling law for the correlation time [4–6]:

$$t_{\text{corr}} = \frac{b\rho_m L}{\langle\dot{\gamma}\rangle}, \tag{4}$$

where L is the average slip line length and ρ_m the density of mobile dislocations.

The present stochastic dislocation dynamics is based on the idea that dislocation glide occurs in a *fluctuating effective medium* that is made up by the ensemble of dislocations. The scaling relations (1)–(4) are supposed to reflect those aspects of long-range dislocation interactions that are relevant on a mesoscopic scale. They represent the starting point for formulating mesoscopic stochastic differential equations of the Langevin type for the evolution of the mechanical and microstructural variables characterizing plastic flow. Thereby it turns out that the stochastic approach opens up new relationships that cannot be obtained from deterministic approaches.

2. APPLICATIONS

2.1. Deformation inhomogeneities

On a mesoscopic scale, fluctuations are quite significant even if the macroscopic plastic deformation proceeds smoothly. In the case of weakly rate-sensitive face-centred cubic (f.c.c.) metals (where S is very small as compared to $\langle\tau^{\text{int}}\rangle$), Eqs. (1), (2) predict large local strain-rate fluctuations of the order of $\langle\delta\dot{\gamma}^2\rangle/\langle\dot{\gamma}\rangle^2 \approx 10^2$ to 10^3, which is consistent with the observation of a coarse mode of slip (formation of slip bands [8]). It is commonly assumed that the fluctuations average

out efficiently so that they do not significantly influence the plastic deformation behaviour of a macroscopic tensile specimen. While this is quite well fulfilled in the case of a polycrystal where the deformation is brought about by an enormous number of independent slip events within different crystallites, it has been shown that fluctuations are appreciable in the deformation of single crystals [9-11], as slip tends to spread within slip bands extending over the entire specimen cross section. In particular, this is true when one approaches a strain-rate softening regime ($S \to 0$) that goes along with a diverging correlation length ξ [12, 13].

The fluctuations of the elongation rate $\dot{l}$ of a macroscopic specimen (or specimen segment) of length l deforming by single-slip follow from Eqs. (1) and (3) as

$$\langle \delta \dot{l}^2 \rangle = \frac{1}{M^2} \int_0^l \int_0^l \langle \delta\dot{\gamma}(x)\delta\dot{\gamma}(x') \rangle \, \mathrm{d}x\mathrm{d}x' \approx \frac{2\xi'l}{M^2} \langle \delta\dot{\gamma}^2 \rangle, \tag{5}$$

or with the tensile strain rate $\dot{\epsilon} = \dot{l}/l$

$$\frac{\langle \delta\dot{\epsilon}^2 \rangle}{\langle \dot{\epsilon} \rangle^2} = \frac{\langle \delta\dot{l}^2 \rangle}{\langle \dot{l} \rangle^2} = 2\frac{\xi'}{l}\frac{\langle \delta\dot{\gamma}^2 \rangle}{\langle \dot{\gamma} \rangle^2} = 2\frac{\xi'}{l}\frac{\langle \tau^{\text{int}} \rangle}{S}. \tag{6}$$

Here ξ' is the projection of ξ on the tensile axis and M is the Schmid factor of the primary slip system. The correlation time of the elongation-rate fluctuations equals that of the underlying mesoscopic strain-rate fluctuations, Eq. (4). In polycrystals, because of the independence of the strain-rate fluctuations within different crystallites, the macroscopic elongation-rate fluctuations are reduced by a factor of $(d/r)^2$, where d is the grain size and r the specimen radius. Taking a typical grain size of 100 μm and a specimen radius of 3 mm, one has $(d/r)^2 \approx 10^{-3}$, i.e., macroscopic fluctuations play much less a role in polycrystals than in single crystals.

2.1.1. Macroscopic strain fluctuations

Considering an ensemble of statistically equivalent specimen segments, we may define by $E = \epsilon - \bar{\epsilon} = (l - \langle l \rangle)/l_0$ the deviations of the segment strains, E, from the average strain $\bar{\epsilon}$ of all segments (l_0 is the initial segment length). Assuming that (i) the slip activity only depends on the mean strain $\bar{\epsilon}$ regardless of the actual strain accumulated locally and that (ii) fluctuations of the macroscopic strain rate result from many, statistically independent events (slip bands), the strain deviation E is subjected to a Wiener process [14, 15],

$$\frac{\mathrm{d}E}{\mathrm{d}\bar{\epsilon}} = \sqrt{2D_\epsilon}\, w(\bar{\epsilon}), \tag{7}$$

with a standard white noise $w(\bar{\epsilon})$ defined by

$$\langle w(\bar{\epsilon}) \rangle = 0, \quad \langle w(\bar{\epsilon})w(\bar{\epsilon}') \rangle = \delta(\bar{\epsilon} - \bar{\epsilon}') \tag{8}$$

and a fluctuation strength that is characterized by the pseudodiffusion coefficient

$$D_\epsilon = \frac{1}{2} \frac{\langle \delta \dot{l}^2 \rangle}{\langle \dot{l} \rangle^2} t_{\text{corr}} \langle \dot{\epsilon} \rangle = \frac{\xi' \langle \tau^{\text{int}} \rangle}{l} \frac{\rho_m b L}{S} \frac{}{M} . \tag{9}$$

The solution of this standard problem of statistical mechanics follows from solving the corresponding Fokker–Planck equation for the probability density $p(E, \bar{\epsilon})$,

$$\frac{\partial}{\partial \bar{\epsilon}} p(E, \bar{\epsilon}) = D_\epsilon(\bar{\epsilon}) \frac{\partial^2}{\partial E^2} p(E, \bar{\epsilon}) , \tag{10}$$

for the initial condition that all specimen segments are undeformed at zero mean strain: $p(E, \bar{\epsilon} = 0) = \delta(E)$. The strain deviations are then Gaussian distributed with a mean square deviation that broadens during straining in a diffusion-like way:

$$\langle E^2 \rangle = 2 \int D_\epsilon(\bar{\epsilon}) \, d\bar{\epsilon} . \tag{11}$$

In the case of a constant fluctuation strength D_ϵ that follows for deformation conditions where the Cottrell–Stokes law holds (i.e., $\langle \tau^{\text{int}} \rangle \sim S, L \sim \xi \sim \rho_m^{-1/2} \sim \langle \tau^{\text{int}} \rangle^{-1}$, see [16]), Eq. (11) reduces to $\langle E^2 \rangle = 2 D_\epsilon \bar{\epsilon}$, that is, the strain variance increases in proportion to the square root of the mean strain (random walk). This result can also be derived in a more mechanistic way by assuming that the strain is accommodated by a certain number of random, discrete, simultaneously active slip events that on average last a time t_{corr} and bring in an elementary strain $\Delta \epsilon$ [10].

Figure 3 presents a comparison with experimental investigations performed by Diehl [17] who monitored the inhomogeneity of tensile deformation by marking five segments with the length 6 mm each on the gauge length of a monocrystalline copper specimen. One notes that in Stage II of strain hardening [18] the variance of the segment strains is well represented by a $\sqrt{\bar{\epsilon}}$-relationship with $D_\epsilon \approx 7.5 \times 10^{-4}$ – a value that is consistent with what one expects from Eq. (9). This is an indication that the assumptions made above (statistical independence of slip events, and validity of the Cottrell–Stokes law) represent good approximations to the actual hardening dynamics during Stage II. In Stages I and III, however, the observed statistics differ systematically from what is expected for constant D_ϵ, demonstrating that deformation mechanisms are different there: The observed decrease of the strain variance in Stage I is consistent with a self-avoiding mode of slip, i.e., the crystal fills up continuously with slip lines that harden a surrounding material slice. This violates the assumed statistical independence of events. On the other hand, in Stage III the strain variance turns out to be constant within the statistical limits of confidence of the experimental data. This may be explained by assuming that at the end of Stage II the pseudodiffusion coefficient D_ϵ drops markedly. This assumption is consistent with current theories which attribute Stage III to the onset of abundant cross slip [19, 20]. By providing an additional degree of freedom, cross slip reduces the strain-rate fluctuation amplitude [4], corresponding to a marked drop in D_ϵ.
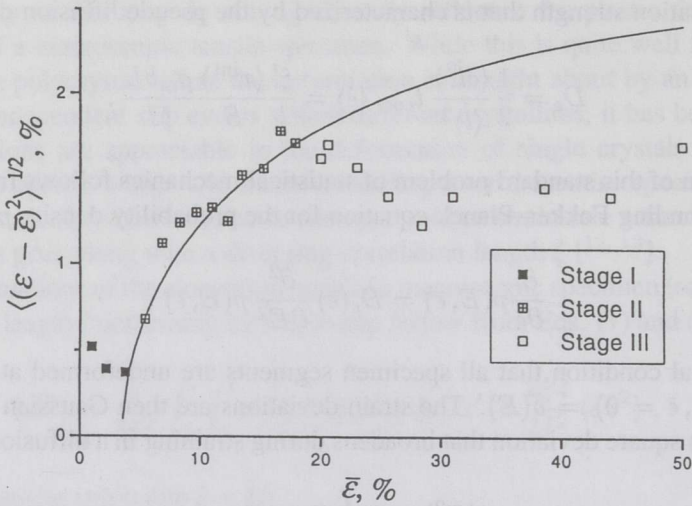
Fig. 3. The variance of the plastic strains of macroscopic specimen segments as a function of the total plastic strain, demonstrating the diffusion-like behaviour of plastic deformation by single glide (Eq. (11)); experimental data for Cu deformed at room temperature, after Diehl [17].

2.1.2. Macroscopic stress fluctuations

Let us now turn to the fluctuations of the external tensile stress σ^{ext} which can be determined by a stochastic integration similar to that used before for the plastic strain. Using the machine equation that relates the imposed cross-head velocity u to the overall plastic strain rate and the elastic strain rate (C denotes the compliance of the system specimen–tensile machine),

$$u = \frac{1}{M} \int_0^l dx\, \dot{\gamma} + Cl\, \dot{\sigma}^{\text{ext}}, \tag{12}$$

one finds for temporal fluctuations of the tensile stress rate [10]

$$\frac{\langle (\delta \dot{\sigma}^{\text{ext}})^2 \rangle}{\langle \dot{\sigma}^{\text{ext}} \rangle^2} = \frac{1}{(C\theta)^2} \frac{\langle \delta \dot{l}^2 \rangle}{\langle \dot{l} \rangle^2}, \tag{13}$$

where $\theta = \langle \dot{\sigma}^{\text{ext}} \rangle / \langle \dot{\varepsilon} \rangle$ is the macroscopic strain hardening coefficient.

Since $C\theta \ll 1$ for a stiff tensile machine, the relative stress rate fluctuations may be appreciable. This is, however, not necessarily true for the corresponding relative deviations of the stress itself. The reason is that the stress is forced to stay close to its expectation value by two intrinsic mechanisms that are related to the fact that the external stress and the flow stress are not independent from each other: (i) The duration t_c of a stress deviation originating from a mesoscopic inhomogeneity of the slip activity is delimited by the global response of the machine–specimen

system [10]: $t_c = CMS/\langle\dot{\epsilon}\rangle$. (ii) Any lasting deviation of the external stress must be realized on the microstructural level in terms of a corresponding strain hardening/softening, so that the average external stress equals the macroscopic flow stress of the material. Spatio-temporal deviations of the flow stress can only be sustained during the activity of a slip band, i.e., on a time scale on the order of $t_{corr} = b\rho_m L/M\langle\dot{\epsilon}\rangle$. Therefore, the external stress cannot depart from its expectation value by performing a random walk.

Again, the temporal evolution of the deviations of the external stress, $\Sigma = \sigma^{ext} - \bar{\sigma}^{ext}$, can be described by a stochastic differential equation which, in the present case, possesses the form of a Langevin equation:

$$\frac{d\Sigma}{d\bar{\epsilon}} = \sqrt{2D_\sigma}\, w(\bar{\epsilon}) - \frac{\Sigma}{\epsilon_{corr}}, \tag{14}$$

where $\epsilon_{corr} = \langle\dot{\epsilon}\rangle\, t_{corr} = b\rho_m L/M$ is the characteristic strain associated with the correlation time, and where the diffusion-like coefficient D_σ is given by [10]

$$D_\sigma = \frac{t_c}{2\langle\dot{\epsilon}\rangle}\langle(\delta\dot{\sigma}^{ext})^2\rangle. \tag{15}$$

The corresponding Fokker–Planck equation for the probability distribution $p(\Sigma, \bar{\epsilon})$ is now of the drift–diffusion type:

$$\frac{\partial}{\partial\bar{\epsilon}} p(\Sigma, \bar{\epsilon}) = D_\sigma \frac{\partial^2}{\partial\Sigma^2} p(\Sigma, \bar{\epsilon}) + \frac{\partial}{\partial\Sigma}\left(\frac{\Sigma}{\epsilon_{corr}} p(\Sigma, \bar{\epsilon})\right), \tag{16}$$

with the steady-state solution

$$p_s(\Sigma, \bar{\epsilon}) = \frac{1}{\sqrt{2\pi D_\sigma \epsilon_{corr}}} \exp\left[-\frac{\Sigma^2}{2D_\sigma \epsilon_{corr}}\right]. \tag{17}$$

Using material parameters typical of a f.c.c. metal deformed in single slip orientation by a stiff tensile machine, one finds the stress fluctuations to be close to the percent range [10]. Particularly pronounced stress fluctuations are encountered with dilute alloys showing dynamic strain ageing [12]. In a certain range of temperature, strain, and strain rate, this may give rise to a strain-rate softening instability ($S = 0$) that comes along with serrated flow (Portevin–Le Châtelier effect [12, 13, 21]). Equations (13), (15), (17) can be used to study the collective dislocation behaviour and *critical stress fluctuations* that occur when S tends to zero [10, 13].

2.2. Noise-induced dislocation patterning

In the following, we shall outline some implications of the stochastic approach regarding the spontaneous formation of dislocation patterns. In doing so we

shall first introduce some basic notions of the theoretical framework of noise-induced transitions [15], and then briefly discuss two applications to dislocation patterning during (i) unidirectional and (ii) cyclic plastic deformation. To keep the representation as simple as possible, let us assume that an emerging dislocation pattern can be described in terms of a single-order parameter ρ which, in general, will be identified with the density of the *immobile* dislocations accumulated during the plastic deformation (e.g. dislocation tangles or sessile dislocation dipoles). Since the systematic evolution of ρ proceeds on a much slower time scale than that of the *mobile* dislocation density ρ_m, we may assume that the latter has been eliminated adiabatically. If, in addition, we neglect any static recovery processes, all dislocation reaction rates considered are in proportion to the plastic shear strain rate $\dot{\gamma}$. Under these circumstances, the evolution equation for ρ assumes the general form

$$\partial_t \rho = f(\rho)\langle\dot{\gamma}\rangle + \sigma\, g(\rho)\, \delta\dot{\gamma} \qquad (18)$$

with the (appropriately scaled) plastic strain rate $\dot{\gamma} = \langle\dot{\gamma}\rangle + \delta\dot{\gamma}$ split into its mean value $\langle\dot{\gamma}\rangle$ and a fluctuating part $\delta\dot{\gamma}$ with zero mean value. The first term on the right-hand side of this generalized Langevin equation describes the systematic evolution as in the deterministic case. The second term represents the noise which, in general, is *multiplicative*, as the random force depends on the dynamic variable ρ. Under these circumstances noise-induced transitions may show up [15].

The fluctuating terms of Eq. (18) are the price to pay for neglecting the microscopic details of transient dislocation interactions in favour of a mesoscopic effective medium description that treats the interaction dynamics as an intrinsic noise. In order to analyse the probability of a certain state as characterized by ρ and investigate the signature of dislocation patterning in probability space, Eq. (18) is transformed into the corresponding Fokker–Planck equation for the transition probability density. Using the Stratonovich calculus, one gets [15]

$$\partial_t p = -\partial_\rho \left[\left(f(\rho)\langle\dot{\gamma}\rangle + \frac{\sigma^2}{4}\partial_\rho g^2(\rho) \right) p \right] + \frac{\sigma^2}{2}\partial_\rho^2 \left[g^2(\rho)\, p \right], \qquad (19)$$

where $p = p(\rho, t \,|\, \rho_0, t_0)$ denotes the probability to find the system in the state ρ at time t, when it was in ρ_0 at t_0, and σ^2 is a measure of the noise intensity that is in proportion to the correlation time. Note that for the derivation of the Fokker–Planck equation (19), the strain-rate fluctuations have been approximated by a Gaussian white noise. This is possible, since the time scale of fluctuations is small as compared to the time scale of the systematic system's evolution (governed by strain hardening). For the same reason one may obtain all information relevant to dislocation patterning by investigating the steady-state distribution function $p_s(\rho)$ as a parametric function of the slowly varying mechanical quantities, such as the flow stress and the strain-rate sensitivity. These aspects are considered important technical advantages of the stochastic dislocation dynamics.

Provided that the probability current vanishes at the boundaries of ρ, the steady-state solution of Eq. (19) reads:

$$p = p_{\mathrm{s}}(\rho) = \frac{\mathcal{N}}{g(\rho)} \exp\left(\frac{2\langle\dot{\gamma}\rangle}{\sigma^2} \int_0^\rho d\rho' \frac{f(\rho')}{g^2(\rho')}\right), \tag{20}$$

where $\mathcal{N}$ is a normalization constant. A noise-induced transition may manifest itself by (i) the loss of integrability of $p_{\mathrm{s}}(\rho)$ occurring at some critical noise level (for an example pertinent to the formation of slip channels see [22]) or by (ii) a qualitative change in shape of $p_{\mathrm{s}}(\rho)$. In the remainder of this paper two examples belonging to the latter category will be presented.

2.2.1. Dislocation cell structures

Cellular dislocation structures are commonly observed to form when dislocations of various slip systems interact with each other (multiple slip). The average cell size λ is known to scale as the inverse square root of the total dislocation density which, in turn, behaves as the square of the flow stress (principle of similitude: $\lambda \sim \rho^{-1/2} \sim (\tau^{\mathrm{ext}})^{-1}$) [23]. To describe this patterning phenomenon, a simple model equation of the type introduced above (Eq. (18)) has been adopted with $f(\rho) = 1 - \sqrt{\rho}$ accounting for dislocation generation and annihilation, and $g(\rho) = \phi + \sqrt{\rho}$, [6]. The dimensionless average effective stress ϕ is the only material parameter besides the scaled noise intensity σ^2.
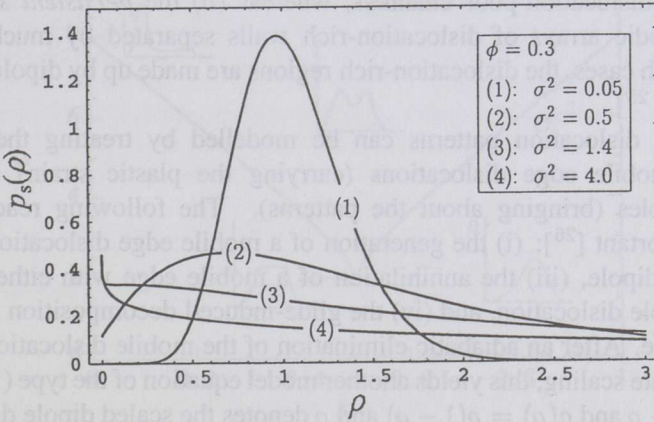
Fig. 4. Probability distributions of the total dislocation density pertinent to the formation of dislocation cell structures (see text).

A straightforward analysis presented elsewhere [6] gives the probability distributions of the total dislocation density ρ in dependence of the parameters σ^2 and ϕ, a typical example of which is shown in Fig. 4. As one expects, the distribution is smeared out around the deterministic steady state $\rho = 1$ at small values of σ^2. At some critical value $\sigma^2 = \sigma_c^2$ (about 1.4 in the specific example),

the maximum of $p_s(\rho)$ gives way to an inflection point with horizontal tangent and a cusp appears at $\rho = 0$ corresponding to the emergence of dislocation free regions (i.e. the interiors of dislocation cells). At the same time the distributions become very broad, which is consistent with the observation that cell formation does not go along with *periodic* patterning, but with a *hierarchical* spectrum of dislocation densities.

In dimensional terms, the model allows for explaining several basic observations. The critical condition $\sigma^2 > \sigma_c^2$ is found to be fulfilled if the correlation length ξ (Eq. (3)) exceeds the average spacing of mobile dislocations, $\rho_m^{-1/2}$. This is an indication that cell formation represents a collective dislocation dynamics effect. The principle of similitude is recovered if we note that the Cottrell–Stokes law holds ($\xi \sim (\tau^{\text{ext}})^{-1}$) and identify ξ with the average characteristic coherence length of the cellular structure. Moreover, the model allows one to attribute the absence of cell formation in body-centred cubic metals deformed at low temperatures to the large strain-rate sensitivity S and the correspondingly small strain-rate fluctuations observed there.

2.2.2. Fatigue dislocation patterning

Ordered dislocation structures are also found in f.c.c. metals fatigued by strain-controlled cyclic plastic deformation (see the electron micrograph on the right part of Fig. 2). Two types of structures may be distinguished: (i) the so-called *matrix structure* consists of more or less regularly arranged dislocation-rich veins embedded into dislocation-poor channels, whereas (ii) the *persistent slip bands* (PSB) are periodic arrays of dislocation-rich walls separated by much broader channels. In both cases, the dislocation-rich regions are made up by dipoles of edge dislocations [24, 25].

The fatigue dislocation patterns can be modelled by treating the coupled dynamics of mobile edge dislocations (carrying the plastic strain) and edge dislocation dipoles (bringing about the patterns). The following reactions are considered important [26]: (i) the generation of a mobile edge dislocation, (ii) the formation of a dipole, (iii) the annihilation of a mobile edge with either another mobile or a dipole dislocation, and (iv) the glide-induced decomposition (breaking apart) of a dipole. After an adiabatic elimination of the mobile dislocation density and an appropriate scaling, this yields another model equation of the type (18) where now $f(\rho) = \kappa - \rho$ and $g(\rho) = \rho(1 - \rho)$ and ρ denotes the scaled dipole dislocation density. The parameter κ represents the dimensionless dipole formation rate. Note that the cyclic nature of plastic deformation is taken into account by identifying the correlation time (which enters the noise intensity σ^2) with the cycle period [26].

Figure 5 shows two sets of probability distributions of the dipole density for $\kappa = 0.3$ and $\kappa = 0.5$, respectively. In both cases the distributions are seen to change from monomodal to bimodal ones, as the noise intensity σ^2 exceeds some critical value. This is indicative of a phase separation into dipole-rich regions (veins and walls) and dipole-poor regions (channels). As to the relative volume fractions,

one notes that $\kappa < 0.5$ gives rise to PSB-like structures with channels occupying a higher volume fraction than walls. $\kappa = 0.5$ represents a situation where the probability distributions are symmetrical with respect to $\rho = 0.5$ and the relative volume fractions are equal. This corresponds to matrix structures with equal volume fractions of veins and channels [26].
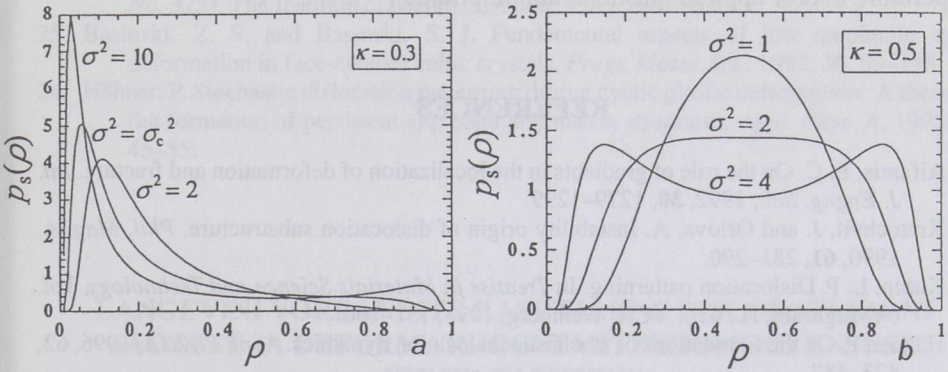
Fig. 5. Probability distributions of the dipole dislocation density pertinent to the formation of persistent slip band structures (*a*) and matrix structures (*b*); for details see text.
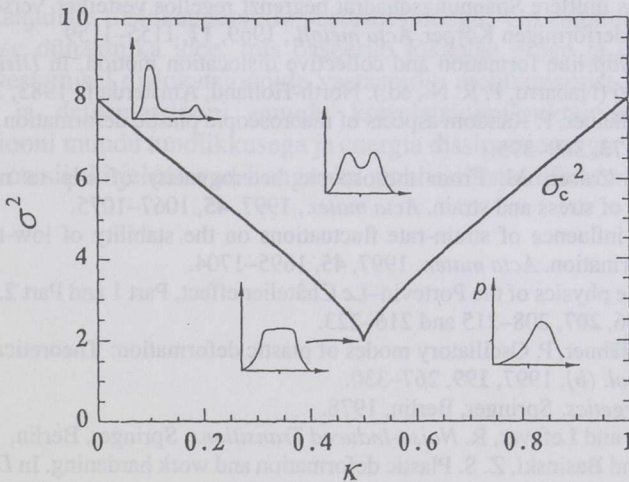
Fig. 6. Phase diagram of fatigue dislocation patterning in dependence of the noise intensity σ^2 and the dipole generation rate κ. Above the cusp-like phase boundary σ_c^2, dislocation patterning occurs, since distribution functions are bimodal.

A phase diagram is given in Fig. 6. From the shape of the phase boundary σ_c^2, separating monomodal dipole distributions from bimodal ones, we infer that $\kappa = 0.5$ represents a particular case. This may explain why fatigue dislocation patterning always commences by the formation of a matrix structure, while PSBs

may eventually form in a later stage of cyclic deformation. The details of the temporal evolution of the dipole patterns can be investigated by considering strain hardening trajectories in $\{\sigma^2, \kappa\}$ phase space [26]. Here we only mention that the model gives (i) the strain amplitudes localized in the PSBs, (ii) the dependence of fatigue patterning on deformation conditions and material parameters, and (iii) the pattern stability against, or the characteristic changes during, changes of temperature and/or applied plastic strain amplitude [26].

REFERENCES

1. Aifantis, E. C. On the role of gradients in the localization of deformation and fracture. *Int. J. Engng. Sci.*, 1992, **30**, 1279–1299.
2. Kratochvil, J. and Orlova, A. Instability origin of dislocation substructure. *Phil. Mag. A*, 1990, **61**, 281–290.
3. Kubin, L. P. Dislocation patterning. In *Treatise in Materials Science and Technology, Vol. 6* (Mughrabi, H., ed.). VCH, Weinberg, 1993, 137–190.
4. Hähner, P. On the foundations of stochastic dislocation dynamics. *Appl. Phys. A*, 1996, **62**, 473–482.
5. Hähner, P. Stochasticity in dislocation dynamics: An effective-medium approach to plastic deformation phenomena. In *Continuum Models and Discrete Systems 8* (Markov, K. Z., ed.). World Scientific, Singapore, 1996, 514–521.
6. Hähner, P. A theory of dislocation cell formation based on a stochastic dislocation dynamics. *Acta mater.*, 1996, **44**, 2345–2352.
7. Wilkens, M. Das mittlere Spannungsquadrat begrenzt regellos verteilter Versetzungen in einem zylinderförmigen Körper. *Acta metall.*, 1969, **17**, 1155–1159.
8. Neuhäuser, H. Slip-line formation and collective dislocation motion. In *Dislocations in Solids, Vol. 6* (Nabarro, F. R. N., ed.). North-Holland, Amsterdam, 1983, 319–440.
9. Zaiser, M. and Hähner, P. Random aspects of macroscopic plastic deformation. *Phil. Mag. Lett.*, 1996, **73**, 369–375.
10. Hähner, P. and Zaiser, M. From mesoscopic heterogeneity of slip to macroscopic fluctuations of stress and strain. *Acta mater.*, 1997, **45**, 1067–1075.
11. Zaiser, M. The influence of strain-rate fluctuations on the stability of low-temperature plastic deformation. *Acta mater.*, 1997, **45**, 1695–1704.
12. Hähner, P. On the physics of the Portevin–Le Châtelier effect, Part 1 and Part 2. *Mater. Sci. Eng. A*, 1996, **207**, 208–215 and 216–223.
13. Zaiser, M. and Hähner, P. Oscillatory modes of plastic deformation: Theoretical concepts. *phys. stat. sol. (b)*, 1997, **199**, 267–330.
14. Haken, H. *Synergetics.* Springer, Berlin, 1978.
15. Horsthemke, W. and Lefever, R. *Noise-Induced Transitions.* Springer, Berlin, 1994.
16. Basinski, S. J. and Basinski, Z. S. Plastic deformation and work hardening. In *Dislocations in Solids, Vol. 4* (Nabarro, F. R. N., ed.). North-Holland, Amsterdam, 1979, 261–362.
17. Diehl, J. Zugverformung von Kupfer-Einkristallen, Teil 1 und Teil 2. *Z. Metallkde.*, 1956, **47**, 331–343 and 411–416.
18. Nabarro, F. R. N. Work hardening of face-centered cubic single crystals. In *Strength of Metals and Alloys (ICSMA 7), Vol. 3* (McQueen, H. J. et al., eds.). Pergamon Press, Oxford, 1985, 1667–1700.
19. Seeger, A. The mechanism of glide and work hardening in face-centred cubic and hexagonal close-packed metals. In *Dislocations and Mechanical Properties of Crystals* (Fisher, J. C. et al., eds.). Wiley, New York, 1957, 243–332.
20. Zaiser, M. and Hähner, P. Hardening-stage III revisited. *Acta mater.*, 1997 (submitted).

21. Hähner, P. Modelling the spatio-temporal aspects of the Portevin–Le Châtelier effect. *Mater. Sci. Eng. A*, 1993, **164**, 23–34.
22. Zaiser, M. and Hähner, P. A theory of the formation of slip channels in cold-worked body-centred cubic metals. *Phil. Mag. A*, 1996, **74**, 287–298.
23. Raj, S. V. and Pharr, G. M. A compilation and analysis of data for the stress dependence of the subgrain size. *Mater. Sci. Eng.*, 1986, **81**, 217–237.
24. Mughrabi, H. Dislocations in fatigue. In *Dislocations and Properties of Real Metals (Book No. 323)*. The Institute of Metals, London, 1985, 244–262.
25. Basinski, Z. S. and Basinski, S. J. Fundamental aspects of low amplitude cyclic deformation in face-centred cubic crystals. *Progr. Mater. Sci.*, 1992, **36**, 89–148.
26. Hähner, P. Stochastic dislocation patterning during cyclic plastic deformation: A theory of the formation of persistent slip band and matrix structures. *Appl. Phys. A*, 1996, **63**, 45–55.

LANGEVINI VÕRRANDITE KASUTAMINE DISLOKATSIOONI JAOTUSE JA DEFORMATSIOONI MITTEHOMOGEENSUSE KIRJELDAMISEKS

Peter HÄHNER

Ajalis-ruumiliste struktuuride teke plastse voolamise tingimustes on seotud pikaajaliste dislokatsioonide vastasmõjudega. On esitatud dislokatsioonide stohhastilise dünaamika idee, mis baseerub lokaalse pinge ja plastse nihkepinge muudu arvestamisel dislokatsioonide vastasmõju mehhanismist lähtudes.

Pinge ja deformatsiooni muudu korrelatsioonifunktsioonid on seostatud deformatsiooni muudu tundlikkusega ja energia dissipatsiooniga. Plastse voolamise omadused on siis kirjeldatavad Langevini stohhastiliste diferentsiaalvõrranditega.